DESIGN AND OPERATING CHARACTERISTICS OF A CW NON-SYNCHRONOUS TRAVELING WAVE STRUCTURE FOR A 900 MeV PULSE STRETCHER RING

J. Haimson and B. Mecklenburg
Haimson Research Corporation
4151 Middlefield Road • Palo Alto California 94303-4793

Abstract

The advantages of using a low loss, high group velocity TW circuit in pulse stretcher ring applications to compensate for synchrotron radiation and parasitic losses over a wide range of beam loading conditions and to control beam spill over a wide energy range are discussed, and details of a cw 2856 MHz TW microwave structure designed to satisfy the operating requirements of the 900 MeV pulse stretcher ring at NIKHEF-K, Amsterdam[1] are presented. The design and operating characteristics of the TW structure for this pulse stretching application are shown tabulated and graphed for a wide range of beam energy and beam loading conditions. The higher order mode (HOM) extraction, absorption and incoherency de-Q-ing techniques used in the design and fabrication of the overall assembly are described, and extracted RF signal waveforms identifying the HOM resonances are also presented.

Introduction

The concept and design philosophy of using a high group velocity, non-synchronous cw traveling wave structure in a pulse stretcher ring (PSR) to accurately compensate for synchrotron radiation and parasitic losses and to control the beam spill over a wide range of operating energies and currents to maximize the effective duty cycle of the extracted beam, have been described elsewhere,[2,3,4] and the operational advantages of these asynchronous TW structures are summarized below.

(a) The PSR can be operated over a wide range of beam energies and pulse currents without requiring the structure to have adjustable RF coupling and tuning controls. This is made possible because the multi-cavity, broad band TW structure presents a matched impedance (VSWR $=1.05$ to 1.10) to the RF source over the full range of beam loading, and the non-synchronous interaction enables beam induced reactive phase shifts to be fully compensated by combining the (fixed tune) counter phase slip of the structure with a small trim adjustment of a low level (digital) phase shifter in the klystron drive circuit.

(b) Special temperature compensation controls are unnecessary because the structure resonant condition is automatically maintained as the cw input RF power is varied over the full operating range. This is made possible by using multiple internal cooling channels and a very low dissipation circuit (less than 60W per cavity).

(c) The use of a very large beam aperture design, to satisfy the ring lattice admittance requirements, enables the structure to be operated at the same resonant frequency as the injector linac and simultaneously provides a fast RF filling time ($\approx$20 ns). This latter feature results in a highly phase stable circuit that is insensitive to normal variations of temperature and frequency (refer Table II), provides a fast response capability so that abrupt phase shift or amplitude control techniques can be employed to optimize the extracted beam duty factor, and minimizes troublesome RF transients that can be associated with fast beam injection into the ring.

(d) For a given operating condition, rapid and precise control of the beam energy can be achieved in a single orbit period of the PSR without altering the input RF power level by adjustment (digital control) of the input RF phase to the TW structure. Since the beam energy gain is highly dependent on this adjustment, accurate control of the cavity input phase plays an important role in the beam extraction process. (At the University of Saskatchewan PSR, initial operation of the TW structure demonstrated an extracted beam duty factor of 50 percent,[5] and this was subsequently increased to 80 percent by optimizing the RF phase shift control sequence.

In contrast to the advantages summarized above, a detracting feature associated with the use of a cw low gradient, TW structure in PSR applications, is the need to adopt aggressive design and fabrication techniques to minimize the probability of encountering beam induced higher order mode (HOM) instabilities caused by the beam recirculating through the RF cavity several thousand times during the period between injected pulses. These HOM suppression techniques are described in a later Section of this paper.

RF System Parameters

For a given beam energy, the maximum required RF voltage to be provided by the PSR cavity is dependent[3,4] on the RF bucket height, as established by the phase and energy spread of the injected beam, and the ring harmonic number (h) and momentum compaction parameter (α). The synchrotron radiation loss per turn (proportional to the fourth power of beam energy and the reciprocal of the bending radius) is, in general, substantially less than the cavity peak RF voltage, and therefore requires that the bunch centroid be phased relatively close to the RF zero crossing position.

Computed values of the TW structure input power and peak RF voltage are shown plotted versus beam energy and ring orbit loss in Figure 1 for the Amsterdam PSR at a beam loading of 200 mA. These data allow for small additional (parasitic) losses and are based on h and α values[1] of 2016 and 0.027, respectively, and on the use of an energy spectrum compression system at the end of the linac to give an injected energy spread of 0.11 percent.

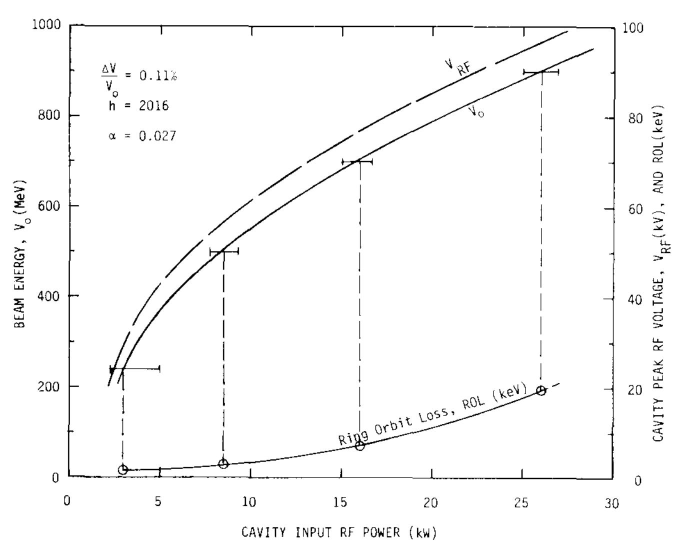

Figure 1. Traveling Wave Structure Input Power and Peak RF Voltage versus Beam Energy and Ring Orbit Loss.

Non-Synchronous Operating Technique

The traveling wave structure was designed to maintain correct compensation for ring losses over a wide range of beam energy and beam loading conditions by phasing the bunch centroid close to the zero crossing while operating in the synchrotron phase stable region. Under these conditions, and especially when operating at reduced beam energies with minimal applied RF power, moderate beam loading can result in large reactive phase shifts.[6] To provide inherent compensation against this effect, the TW structure was designed to have a relative phase velocity (β_w) of less than unity, thereby introducing a counter-phase slip $\psi_0 = 2\pi(z/\lambda)(1-\beta_w)/\beta_w$, where positive values define phase lag with respect to the beam. With this non-synchronous mode of operation, the structure is fixed tuned and resonant at the operating frequency of the linac system; thus, for relativistic particles, the phase slip (ψ_0) is established by the physical dimensions of the circuit only.

For the Amsterdam PSR, ψ_0 was chosen to cause the phase lag of the wave with respect to the beam at high energy, light beam loading conditions to be comparable to the phase advance of the total field vector with respect to the bunch centroid under medium energy, moderately heavy beam loading conditions. With this technique, for any given operating energy and over the full range of beam loading conditions, an entry phase can be selected within a narrow range of values (within 20° of zero crossing) that will result in maintaining the desired beam energy gain to compensate for the ring losses. This is illustrated by the phase orbit and energy gain data shown plotted in Figures 2 and 3 for 50, 100 and 200 mA at beam energy values of 500 and 900 MeV, respectively. For example, in Figure 2, under light beam loading of 50 mA, a bunch centroid entry phase 2½° ahead of the zero crossing results in a structure transit phase advance of 7° to give an energy gain of 3.0 keV; and for heavy beam loading at 200 mA, by advancing the entry phase 16°, a reverse phase slip of 25° occurs during transit of the structure, and the energy gain remains unchanged. The RF structure phase and beam parameter relationships are listed in Table I, and the data shows that the fixed tune phase slip (ψ_0) was chosen to provide near synchronous operation at a median beam energy and beam loading condition. As a general design criteria, for any given operating condition, the required beam energy gain will be maintained constant for different beam loading conditions when the entry phase is selected to maintain a given constant phase value at the midplane of the structure; i.e., a beam loading phase fulcrum point is established at z = L/2. This phase fulcrum point is in advance of the zero crossing by 1, 2½, 5 and 11 degrees, respectively, for the required beam energy gain conditions of 1½, 3, 8 and 20 keV shown in Table I.

TABLE I

Relationship of TW Cavity Entry Phase with Beam Energy and Current

Beam Energy (Mev)	Input Power (kW)	Energy Gain (keV)	Current (mA)	Entry Phase (deg)	Exit Phase (deg)
900	26	20.0	50	8.6	20.3
			100	11.4	17.3
			200	17.4	11.4
700	16	8.0	50	3.7	13.7
			100	7.3	10.0
			200	14.8	2.2
500	8	3.0	→ 50	2.5	9.5
			sync 100	7.6	4.2
			200	18.2	-7.1
250	5	1.5	50	2.7	7.0
			100	9.2	0.2
			200	23.0	-14.2

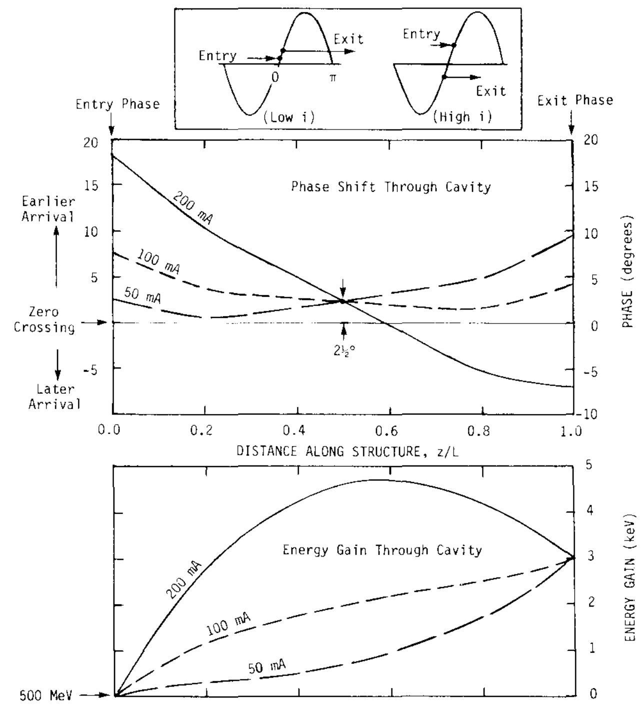

Fig. 2. RF Cavity Phase Shift and Energy Gain vs Distance Along Structure for P_0 =8kW and V_0=500MeV (0.11% ΔV/V).

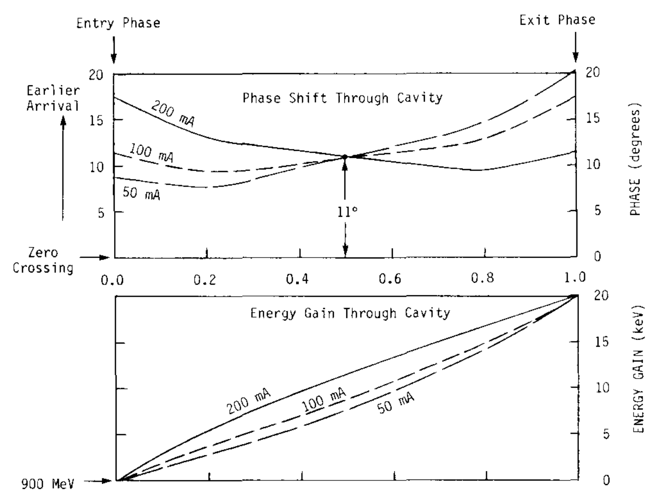

Fig. 3. RF Cavity Phase Orbit and Energy Gain vs Distance Along Structure for P_0=26kW and V_0=900MeV (0.11% ΔV/V).

Description of TW Structure

The RF structure is designed to operate at 2856.0 MHz using twelve 2π/3 mode cavities, including special input and output coupler cavities having large bore re-entrant drift tubes, side wall iris coupling and offset bodies. Two contiguous offset body cavities in the center of the structure are magnetically coupled, in mutually orthogonal planes, to broad band matched WR187 loaded rectangular waveguide circuits for extraction and absorption of higher order modes. The phase velocity of the structure varies from c at the input to 0.976c at the output, to give an unloaded fixed tune phase slip of 17.3 deg. With a minimum diameter beam aperture of 40 mm, the RF insertion loss is 0.12 dB; and at a cw input RF power of 26 kW, the structure dissipation is 708 W at zero beam loading. The total RF filling time of the structure is 21 ns, giving an output phase frequency sensitivity of 7.6 deg/MHz and an output phase/average copper temperature sensitivity of 0.36 deg/°C. The microwave structure design parameters are shown listed in Table II.

TABLE II

TW Structure Design Parameters

Resonant Frequency at 45°C	2856.0 MHz
Traveling Wave Longitudinal Mode	$2\pi/3$
Overall Electrical Length	1440 deg
Beam Aperture Minimum Diameter	40 mm
Input Phase Velocity	1.000c
Output Phase Velocity	0.976c
Fixed Tune Phase Slip of the Unloaded Structure, with respect to c	17.3 deg
VSWR at Resonant Frequency ±3 MHz, less than	1.05:1
RF Insertion Loss	0.12 dB
Structure Copper Losses at an Input Power of 26 kW and Zero Beam Loading	708 W
RF Filling Time	21 ns
Output Phase/Frequency Sensitivity	7.56 deg/MHz
Output Phase/Average Temp. Sensitivity	0.36 deg/°C
Drift Tube Cutoff at 2856 MHz	112 dB

Input and output WR284 rectangular waveguide directional couplers and high power RF window and load assemblies were supplied with the TW structure to form an integrated high vacuum RF system. A view of the system layout including the baseplate and supports and the input and output beam drift tubes is shown in Figure 4. The (27 cm long) beam drift tubes ensure uniform impedance zones, free of collimators, monitors, etc., and enable the HOM field patterns immediately contiguous to the TW structure to be accurately characterized (and reproduced on site), thereby assisting in optimizing the HOM de-Q-ing adjustments.

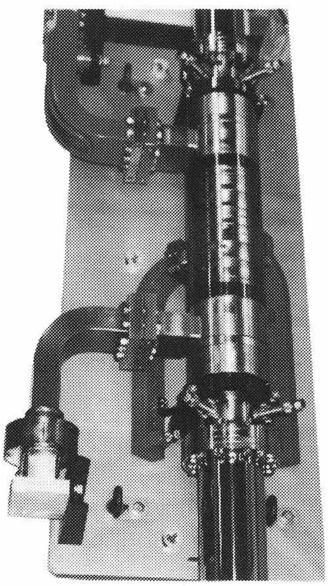

Figure 4.

View of TW Structure Showing Input and Output Beam Drift Tubes and HOM De-Q-ing Features.

De-Q-ing Higher Order Modes

In order to minimize the beam induced HOM field intensities, a variety of previously developed[4] extraction, absorption and incoherence design features were incorporated into this large aperture TW structure. These features included two offset body HOM extraction couplers located in the midsection of the structure and connected to broad band, coaxially terminated, external WR187 E-bend assemblies (refer Figure 4); the use of side wall iris input and output coupler cavities having (tunable) re-entrant high RF loss, slotted drift tube assemblies with a TE_{11} cutoff frequency slightly less than the HEM_{11} lower branch zero mode resonance; the use of externally loaded probes extending into the slotted beam drift tubes and located in two orthogonal planes oriented azimuthally at 45° to the coupler cavity WR284 connections (refer Figure 4); and the use of five different cavity lengths and eight different (2b/2a) cavity diameter ratios.

The effectiveness of coupling the HOM fields, especially the undesirable lower branch[4,7] HEM_{11} modes, from the beam centerline into the matched C-band extraction circuits is illustrated in the Figure 5 waveforms. The waveforms show the frequencies detected at the termination of each WR187 extraction circuit (C_L and C_{SH}) for an RF sweep of 2 to 6 GHz injected into the beam centerline. Similar RF sweep detection measurements also confirmed the effectiveness of coupling the HEM_{11} modes out of the structure through the drift tube beam apertures, and via the wide iris S-band coupler into the WR284 water load. The above techniques resulted in a 15 to 20 dB reduction of the HOM Q values, and HEM_{11} $R_\perp$ upper values of less than 50 kΩ.

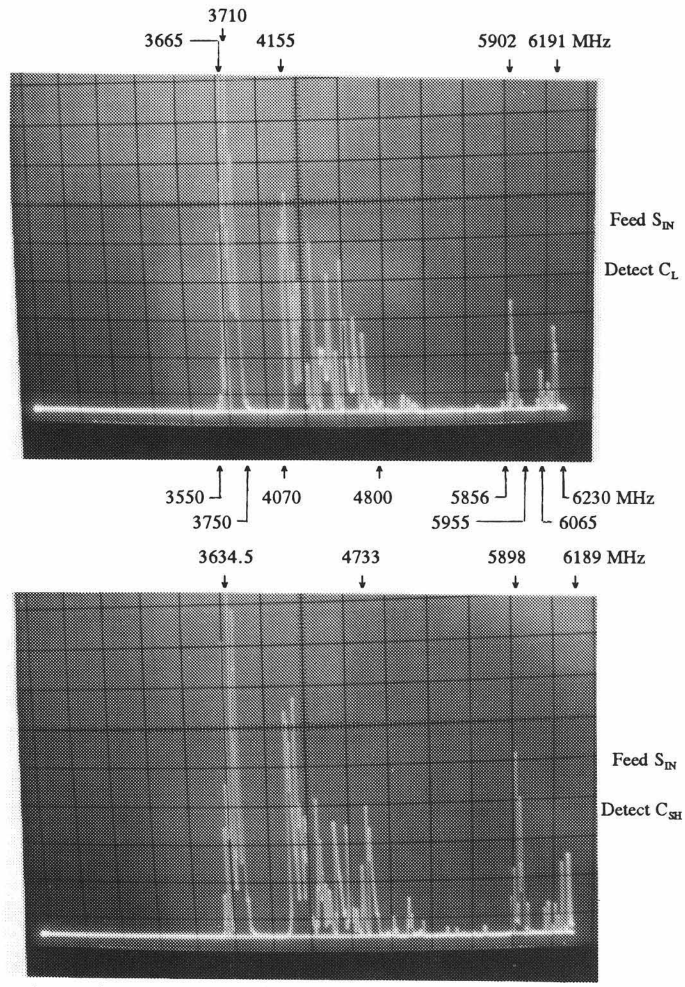

Figure 5. HOM Extraction Circuit Output Signals for a 2 to 6 GHz Swept Excitation of the TW Structure.

References

[1] G. Luijckx, et al., "The Amsterdam Pulse Stretcher Project (AmPS)," Proc. 1989 IEEE Particle Accelerator Conference, Catalog No. 89CH2669-0, pp. 46-48, March 1989.

[2] Haimson Research Corporation Proposal No. HRC-4735, University of Saskatchewan, April 1985.

[3] H.S. Caplan and T.P. Dielschneider, "The RF System for EROS (Electron Ring of Saskatchewan)," SAL Tech. Mem. EROS/TM/PSR/RF/04, September 1985.

[4] J. Haimson and B. Mecklenburg, "A CW Non-Synchronous Traveling Wave Structure for a 300 MeV Pulse Stretcher Ring," Proc. 1987 IEEE Particle Accelerator Conference, Catalog No. 87CH2387-9, pp. 1919-1921, March 1987.

[5] L.O. Dallin, "Operating Results of the Electron Ring of Saskatchewan (EROS)," Proc. 1989 IEEE Particle Accelerator Conference, Catalog No. 89CH2669-0, pp. 22-26, March 1989.

[6] Linear Accelerators, Eds. P. Lapostolle and A. Septier, pp. 432-434, North Holland Pub. Co., Amsterdam, 1970.

[7] J. Haimson and B. Mecklenburg, "Suppression of Beam Induced Pulse Shortening Modes in High Power RF Generator TW Output Structures," Proc. of the SPIE Symposium on Intense Microwave and Particle Beams III, Los Angeles, vol. 1629, pp. 209-219, January 1992.